

# RATDAMPER – A Numerical Model for Coupling Mechanical and Hydrological Properties within the Disturbed Rock Zone at the Waste Isolation Pilot Plant

J.S. Rath  
 Sandia National Laboratories, Carlsbad, New Mexico, USA

T.W. Pfeifle  
 RESPEC Incorporated, Rapid City, South Dakota, USA

U. Hunsche  
 Bundesanstalt für Geowissenschaften und Rohstoffe (BGR), Germany

JT  
 9/22/00  $\left\{ \begin{array}{l} \text{FINAL (Version 6)} \\ 4/14/00 \end{array} \right.$

**ABSTRACT:** A numerical model for predicting damage and permeability in the disturbed rock zone (DRZ) has been developed. The semi-empirical model predicts damage based on a function of stress tensor invariants. For a wide class of problems hydrologic/mechanical coupling is necessary for proper analysis. The RATDAMPER model incorporates dilatant volumetric strain and permeability. The RATDAMPER model has been implemented in a weakly coupled code, which combines a finite element structural code and a finite difference multi-phase fluid flow code. Using the development of inelastic volumetric strain, a value of permeability can be assigned. This flexibility allows empirical permeability functional relationships to be evaluated.

## 1 INTRODUCTION

Sandia National Laboratories (SNL), as the scientific advisor to the Department of Energy (DOE) for the Waste Isolation Pilot Plant (WIPP), is interested in the movement of fluids (e.g., gas and liquid) into and out of the repository horizon and potentially through the panel closures, and sealed vertical shaft systems. The host rock consists of bedded halite, polyhalite, and anhydrite with minor clay seams. Disposal regions are approximately 650m below ground surface, and are mined from the bedded salt of the Salado Formation. Creep closure is a significant technical component of the disposal areas as this phenomenon closes repository rooms, consolidates waste and backfill, thereby influencing performance assessment and seal system designs. The disturbed rock zone (DRZ), formed as a result of damage caused during deformation into excavated openings, causes a measurable change in mechanical and hydrologic properties. For a wide class of problems hydrologic/mechanical coupling is necessary for proper analysis.

The RATDAMPER model has been developed to predict damage and permeability in the DRZ. The semi-empirical model predicts damage based on a function of stress tensor invariants and incorporating dilatant volumetric strain. Laboratory tests using nitrogen gas as the permeant have been conducted to determine permeability of WIPP salt deformed to various levels of damage (Pfeifle 1995, Pfeifle 1998, Pfeifle 1999). From these laboratory tests, several relationships coupling permeability to the development of inelastic strain have been formulated. Most

of the available data focus on small volumetric strains (less than 0.5%). Pfeifle (1999) has recently completed tests that provide additional data for larger volumetric strains ranging from 1 to 2.5%. To avoid function averaging, an approach based on a scalar measure of damage predicts permeability from dilatant behavior observed in laboratory experiments. The damage factor, or a measure of dilatancy,  $D$ , is computed as a function of the second invariant of the deviator stress tensor  $J_2$ , and the first invariant of the stress tensor,  $I_1$ , (Van Sambeek et al. 1993) where

$$D = \frac{\sqrt{J_2}}{(0.27 \cdot I_1)} \quad (1)$$

The use of a stress tensor invariant ratio to measure dilatancy has been previously investigated using WIPP and other rock salt types (Van Sambeek et al. 1993). The scalar quantity,  $D$ , gives a measure of maximum damage that occurs after excavation and does not predict damage evolution.

The RATDAMPER model has been implemented in a weakly coupled code that combines a finite element structural code and a finite difference multi-phase fluid flow code (Statham et al. 1999). Due to complex processes of viscoplastic creep, stress state redistribution and pore pressure effects, this engineering approach is considered an appropriate starting analysis to model the empirical relation between permeability and volumetric strain. Any viable structural code with a constitutive material law simulating rock salt deformation processes might be used to determine the state of stress. Using devel-

## **DISCLAIMER**

**This report was prepared as an account of work sponsored by an agency of the United States Government. Neither the United States Government nor any agency thereof, nor any of their employees, make any warranty, express or implied, or assumes any legal liability or responsibility for the accuracy, completeness, or usefulness of any information, apparatus, product, or process disclosed, or represents that its use would not infringe privately owned rights. Reference herein to any specific commercial product, process, or service by trade name, trademark, manufacturer, or otherwise does not necessarily constitute or imply its endorsement, recommendation, or favoring by the United States Government or any agency thereof. The views and opinions of authors expressed herein do not necessarily state or reflect those of the United States Government or any agency thereof.**

## **DISCLAIMER**

**Portions of this document may be illegible in electronic image products. Images are produced from the best available original document.**

opment of inelastic volumetric strain, a value of permeability can be assigned. This flexibility allows empirical permeability functional relationships to be evaluated.

RECEIVED

NOV 30 2000

OSTI

## 2 APPROACH

The coupling of mechanical and hydrological effects can be quantified according to the principle of effective stress:

$$\sigma_T = pI + \sigma_e \quad (2)$$

Where  $\sigma_T$  is the stress tensor caused by the weight of the overburden (essentially constant),  $p$  is the pressure of the repository pore fluid,  $I$  is the identity tensor, and  $\sigma_e$  is the effective stress tensor that is applied to the matrix. The movement of fluids is directly affected by the hydrologic properties while fluid movement (and resulting fluid pore pressure) directly affects the mechanical processes of salt damage, creep, and healing. Therefore, coupling of fluid flow and rock mechanics would improve the analysis of the movement of fluids in the DRZ surrounding the repository.

## 3 DRZ BEHAVIOR AT WIPP

The degree of rock damage in the DRZ immediately surrounding the excavation is of major importance to the analysis of fluid flow near the repository. Stresses imposed on the host rock during underground excavation, as well as the natural creep of the rock salt into the excavated openings, will cause fracturing in the vicinity of the host rock/repository interface, that will alter the hydrologic properties of the fluid flow system. This DRZ may be hydrologically characterized as having an increased porosity and increased permeability to gas and liquid.

As the underground excavations at WIPP age, large-scale fracturing will develop in the surrounding rock salt, usually becoming visible after several years. The process of fracturing starts immediately after excavation, when deviatoric stresses are at a maximum. Fracturing in the vicinity of the salt rock/repository interface initiates soon after mining begins. Micro-fractures develop at the grain level in response to deviatoric stress changes. Over time, changes in the state of stress resulting from creep displacements promote the coalescence of micro-fractures that become readily visible. A localized, intense fractured pattern forms, leading to larger but fewer fracture zones with preferred orientations controlled by both applied stresses and local stratigraphy (Kranz 1983).

Under certain conditions, such as construction of a rigid bulkhead, stresses in the salt will tend toward

equilibrium. As stress differences decrease, salt fractures would heal.

Inherent to the fracture process is dilatant behavior of the rock mass that results in increased porosity, permeability and a decrease in pore pressure, which leads to an increase in effective stress. Dilatancy, or the volumetric expansion of the rock volume, is therefore a measure of the degree of fracturing and damage in the DRZ. Since the mechanical fracturing processes are time-dependent, it logically follows that the hydrological properties are also time-dependent.

Different levels of fracturing will have varying consequences on the mechanical and hydrological performance of underground openings at WIPP. The scale of the fracturing affects both the porosity and the permeability of the surrounding rock. Micro-fractures significantly increase the permeability of the surrounding rock mass. Subsequent creep alters the state of stress, which continues to change the dilation and permeability in the rock salt.

As fracturing occurs the salt grains will move with respect to each other which, on average, causes rock mass volume expansion. These fractures may heal if the fractured mass is reloaded along the hydrostatic axis (Costin & Wawersik 1980, Brodsky 1990). This is particularly important in rock salt for which fractures can be healed, as the state of stress tries to reach equilibrium. Healing may also occur during deviatoric states of stress, but this is a result of the normal stress components, and not the deviatoric stress itself (Stormont 1995).

Permeability and change in permeability are major parameters in characterizing the DRZ. Permeability is a function of fracturing in a rock salt mass, assuming the salt grains are impermeable. The simplest measure of fracturing and damage is the dilatancy of the rock mass, which is treated as a scalar. Therefore permeability can be related to the mechanical measurements through dilatancy.

## 4 PREVIOUS DILATANCY MODELING AT WIPP

The relationship between dilatancy and permeability in rock salt has been derived from constant confining stress tests on WIPP rock salt (Pfeifle et al. 1998). In these tests, nitrogen gas was used to determine the permeability of a damaged WIPP rock specimen. Stormont (1990) reported the results of a series of compression tests on WIPP salt. During these tests, the permeability of the samples was measured after being subjected to deviatoric loading. Pfeifle (1995) conducted triaxial stress tests on WIPP salt. These triaxial stress tests were run at varying confining pressures,  $\sigma_3$ , and constant stress difference,  $\Delta\sigma$  ( $1.0 < \sigma_3 < 2.5$  MPa, and  $\Delta\sigma = 25$  MPa). These stress tests were terminated after reaching axial strains of

10%. The final volumetric strains for these tests ranged from 1 to 4%. Nitrogen gas permeability testing was then performed on all of the samples. Blankenship (1996) used the data reported by Stormont (1990) and Pfeifle (1995) and fit the data using an exponential function for permeability versus volumetric strain (see Figure 1). Table 1 lists the data fitting functions used in Figure 1. Pfeifle et al. (1998) reported permeability and volumetric strain data from triaxial stress tests on WIPP rock salt, also shown in Figure 1. Assuming that the permeability of intact rock salt is approximately  $1 \times 10^{-21} \text{ m}^2$  (Davies & LaVenue 1990), the permeability changes several orders of magnitude (4 to 7) over a range in dilatant volumetric strain of 0 to 0.5%. Figure 1 shows that permeability changes less rapidly over a range in dilatant volumetric strain from 0.5 to 4%. Triaxial stress tests were recently completed to capture permeability versus dilatant volumetric strain in the dilatant volumetric strain range of 1 to 2.5%, by Pfeifle (1999).

As seen in Figure 1, the Stormont data (WIPP, in-situ) appear to be significantly different than the other experimental data (Pfeifle 1999, Blankenship 1996). These later tests involved cylindrical test specimens subjected to a triaxial state of stress, and then nitrogen gas was injected and permeability was measured.

## 5 NUMERICAL MODEL

### 5.1 Background

Previous WIPP-related analyses have recognized the importance of the interaction between geo-mechanical processes and fluid flow processes in evaluating repository performance. Freeze et al. (1995) summarized several methods for approximating salt creep and disposal room closure in numerical models of multi-phase fluid flow. A method for modeling DRZ healing around the WIPP shaft sealing system is described in RISD (1996). The work done by Freeze et al. (1995) considered the coupling of fluid-flow and mechanical effects indirectly, by using a weak one-way coupling approach. This was accomplished by including pre-defined temporal and spatial relationships between mechanical strain and fluid pressure. This approach does not account for the feedback that dynamically alters the total stress, as shown in equation (2). Freeze et al. (1998) later considered the influence of coupling between mechanical strain and porosity. This study showed that increasing porosity and fracturing can have significant effects on short-term fluid flows. Complete coupling of hydrological and mechanical systems requires two-way coupling. The second coupling mechanism involves the movement of fluids which is directly affected by the hydrologic

properties while fluid movement (and resulting fluid pore pressure) directly affects the mechanical processes of salt damage, creep, and healing. It is likely that formation of the DRZ and salt creep will be influenced by variations in the pore pressure in the immediate vicinity of the repository.

### 5.2 Theory

The scalar damage factor,  $D$ , introduced in equation (1) is used in the RATDAMPER model to relate stress tensor invariants to damage based on dilatant volumetric strain. Generally this stress tensor invariant ratio does not predict evolution of DRZ since it assumes a maximum value immediately following excavation (at which time the extent of the DRZ is actually at a minimum value). Consequently as the stress field relaxes,  $D$  decreases. Although this measure provides a first approximation of damage, the decreasing ratio contradicts the observation that the extent of DRZ continues to develop as the stress field continues to relax. However, the magnitude of  $D$  can be related to dilatancy and provide a first-order means to predict transient permeability of the DRZ.

### 5.3 Procedure

The following three steps present the engineering approach damage-permeability model whereby a region surrounding a portion of the WIPP repository and/or DRZ resides in a numerical computational mesh (or grid) containing elements or grid blocks:

#### Step 1:

The measure of dilatancy,  $D$ , is calculated as:

$$D = \frac{\sqrt{J_2}}{(0.27 \cdot I_1)} = \frac{\sqrt{J_2}}{(0.81 \cdot \sigma_m)} \quad (3)$$

where

$$I_1 = 3 \cdot \sigma_m \quad (4)$$

If  $D \geq 1.0$ , then it is assumed that the element is experiencing dilatant behavior leading to damage (Van Sambeek et al. 1993) and the damage-permeability model can now be applied. If  $D < 1.0$ , then permeability is not changed for the current element.

#### Step 2:

Determine the quantity of dilatant volumetric strain,  $\epsilon_{dv}$ . This requires that "onset of dilatant volumetric strain",  $\epsilon_{odv}$ , be computed first. Hunsche has performed several triaxial stress tests on rock salt similar to WIPP rock salt (Cristescu & Hunsche 1998) and found that the onset of dilatant volumetric strain occurs when the slope of a curve in the octahedral shear stress vs. total volumetric strain plane is vertical. The Cristescu & Hunsche (1998) relation of

octahedral shear stress,  $\tau_{oct}$ , and total volumetric strain,  $\epsilon_{vt}$ , for a given mean stress,  $\sigma_m$ , is shown in Figure 2.

The determination of the dilatant volumetric strain,  $\epsilon_{dv}$ , is as follows:

Determine the total volumetric strain,  $\epsilon_{vt}$ , knowing  $\tau_{oct}$  and  $\sigma_m$  from Figure 2. Table 2 displays  $\tau_{oct}$  as a function of  $\epsilon_{vt}$  for a given  $\sigma_m$ , which correspond to Figure 2. Values in Table 2 were found from Cristescu & Hunsche (1998) and are not representative of WIPP rock salt, but for a similar rock salt. Using the values listed in Table 2, a contour plot of total volumetric strain as a function of both  $\tau_{oct}$  and  $\sigma_m$  is shown in Figure 3. Using the data listed in Table 2, a double linear interpolation provides the total volumetric strain,  $\epsilon_{vt}$ , for a specified  $\tau_{oct}$  and  $\sigma_m$ .

The point at which a curve at constant mean stress,  $\sigma_m$ , in the  $\tau_{oct}$ - $\epsilon_{vt}$  plane has a vertical slope, defines the onset of dilatant volumetric strain,  $\epsilon_{oodv}$ . Figure 2 shows the Octahedral shear stress,  $\tau_{oct}$ , vs. total volumetric strain,  $\epsilon_{vt}$ , for a given mean stress,  $\sigma_m$ . For several mean stress values,  $\sigma_m$ , the points of inflection which correspond to the transition from compressibility to dilatancy of rock salt (or the onset of dilatant volumetric strain,  $\epsilon_{oodv}$ ) are shown in Figure 4. Table 3 lists the  $\tau_{oct}$  and  $\sigma_m$  values at point of inflection (i.e.,  $\epsilon_{oodv}$ ). The functions displayed in Figure 4 are described in detail in Table 4. Using the appropriate function, and knowing the mean stress, the onset of dilatant volumetric strain can easily be computed from

$$\epsilon_{dv} = \epsilon_{oodv} - \epsilon_{vt} \quad (5)$$

### Part 3:

From triaxial stress creep testing of WIPP rock salt (Pfeifle 1997) permeability as a function of dilatant volumetric strain was fitted with two different exponential functions as shown in Figure 1. Using these two empirical permeability functions, and the quantity of dilatant volumetric strain, a new disturbed permeability can be bounded by the Stormont and Blankenship model curves.

Using the dilatant volumetric strain,  $\epsilon_{dv}$ , the corresponding permeability can be found by averaging the Blankenship and Stormont model permeability functions in  $\log_{10}$  space.

## 6 CONCLUSIONS

A damage-permeability model has been developed that is based on a semi-empirical formulation. The engineering approach can be easily implemented into a finite difference or finite element rock mechanics code. A major benefit of the RATDAMPER model is flexibility, such that modifications can be readily accommodated, as new or improved dilatant volumetric strain vs. permeability data become available. This model is an initial step in further development

and research of ongoing DRZ studies, including both numerical calculations and experimental programs. It is expected that such models will provide valuable insight and improved credibility to predict DRZ evolution, which is a key component of current WIPP regulatory compliance requirements.

## 7 ACKNOWLEDGEMENTS

Work performed for Sandia National Laboratories (SNL), which is a multiprogram laboratory operated by Sandia Corporation, a Lockheed Martin Company, for the United States Department of Energy under contract DE-AC04-94-AL85000.

## REFERENCES

- Blankenship, D.A. 1996. "Fitting of RE/SPEC Inc. and Stormont Permeability versus Volumetric Strain Data," prepared by RE/SPEC inc., Rapid City, SD, for Sandia National Laboratories, Albuquerque, NM. Dated January 26, 1996
- Borns, D.J. & J.C. Stormont 1989. *The delineation of the disturbed rock zone surrounding excavations in salt*. Rock Mechanics as a Guide for Efficient Utilization of Natural Resources, Khair (ed.). Rotterdam: A. A. Balkema
- Brodsky, N.S. 1990. "Crack closure and healing studies in WIPP salt using compressional wave velocity and attenuation measurements: test methods and results," SAND90-7076. Sandia National Laboratories: Albuquerque, NM.
- Costin, L.S. & W.R. Wawersik 1980. "Creep Healing of Fractures in Rock Salt," SAND80-0392. Sandia National Laboratories: Albuquerque, NM.
- Cristescu, N.D. & U. Hunsche 1998. "Time Effects in Rock Mechanics," John Wiley & Sons, Chichester, NY.
- Davies, P. & M. LaVenue 1990. Internal Memorandum to Elaine Gorham dated August 01, 1990. "Comments on Model Implementation and Data for Use in August Performance Assessment Calculations". Page 4 [published in Rechard, R.P., H. Iuzzolino & J.S. Sandha 1990. "Data Used in Preliminary Performance Assessment of the Waste Isolation Pilot Plant (1990)", SAND89-2408. Sandia National Laboratories: Albuquerque: NM. Appendix A, memo 3, pg. A-68]
- Freeze, G.A., K.W. Larson & P.B. Davies 1995. "A Summary of Methods for Approximating Salt Creep and Disposal Room Closure in Numerical Models of Multi-phase Flow," SAND94-0251. Albuquerque, NM: Sandia National Laboratories.
- Freeze, G.A., J. Ruskaugg, T.L. Christian-Frear & S.W. Webb 1998. "Modeling the Effect of Excavation-Disturbed Zone Porosity Increase on Groundwater Inflow to an Underground Repository," *Proceedings of the TOUGH Workshop '98*. LBNL-41995. Lawrence Berkeley National Laboratories. Berkeley, CA.
- Kranz R.L. 1983. "Microcracks in rocks: a review" In; M. Freidman and M.N. Toksöz (editors), *Continental Tectonics: Structure, Kinematics and Dynamics*. *Tectonophysics*, 100: 449-480.
- Peach, C.J. 1991. "Influence of Deformation on the Fluid Transport Properties of Salt Rocks," *Geologica Ultraiectina*, ISSN 0072-1027: No. 77, Utrecht, Netherlands

Pfeifle, T.W. 1995. "Progress Report for Sandia National Laboratories Contract AF-3334 Covering Period July 1, 1995 to July 31, 1995," Sandia National Laboratories, August 11, 1995."

Pfeifle, T.W. 1997. "Summary Report on Salt Damage-Versus-Permeability Relationship (Milestone RM101) - FINAL," RSI(RCO)-439/8-97/14.

Pfeifle, T.W., N.S. Brodsky & D.E. Munson 1998. "Experimental Determination of the Relationship Between Permeability and Microfracture-Induced Damage in Bedded Salt" Proceedings, "3<sup>rd</sup> North American Rock Mechanics Symposium, Cancun, Mexico, June 3-5, 1998, published in the International Journal of Rock Mechanics and Mining Sciences, Vol. 35, No. 4/5, Paper No. 042.

Pfeifle T.W. 1999. "Damage Creep Testing of WIPP Salt With Gas Permeability Measurements," RE/SPEC contract AX-9042 with Sandia National Laboratories, Carlsbad, NM

Pruess, K. 1991. "TOUGH2 - A General-Purpose Numerical Simulator for Multi-phase Fluid and Heat Flow," LBL-29400. Berkeley, CA, Earth Sciences Division, Lawrence Berkeley Laboratory.

RISD (Repository Isolation Systems Department). 1996. "Waste Isolation Pilot Plant Sealing System Compliance Submittal Design Report," SAND96-1326/1. Albuquerque, NM: Sandia National Laboratories.

Statham, W.H., M. Reeves, L.D. Hurtado & C.S. Lo 1999. "Coupling of fluid flow and rock mechanics models for analysis of hydraulic performance at the Waste Isolation Pilot Plant," *Proceedings, 9<sup>th</sup> International Congress on Rock Mechanics*, Paris, France, Vol. 2, pp. 965-969.

Stormont, J.C. 1990. "Gas Permeability Changes in Rock Salt During Deformation," Ph.D. Dissertation, University of Arizona, Tucson, AZ.

Stormont, J.C. 1995. "The Influence of Rock Salt Disturbance on Sealing," Second North American Rock Mechanics Symposium, Montreal, Quebec.

Van Sambeek, L.L, J.L. Ratigan & F.D. Hansen 1993 "Dilatancy of Rock Salt in Laboratory Tests," *International Journal of Rock Mechanics, Min. Sci. & Geomech.* Vol. 30, No. 7, pp. 735-738.

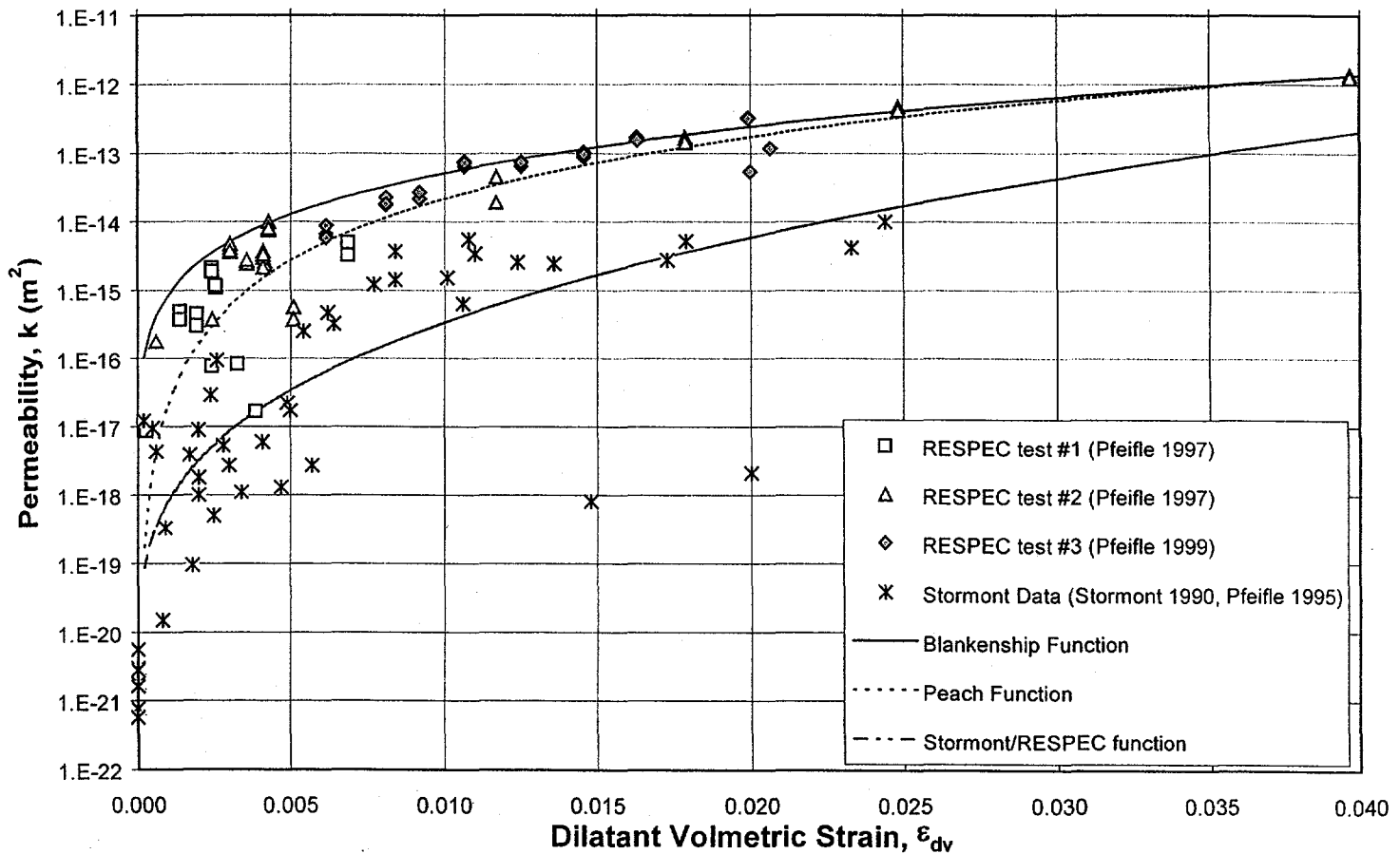


Figure 1. Permeability vs. Dilatant Volumetric Strain ( $k$  vs.  $\epsilon_{dv}$ )

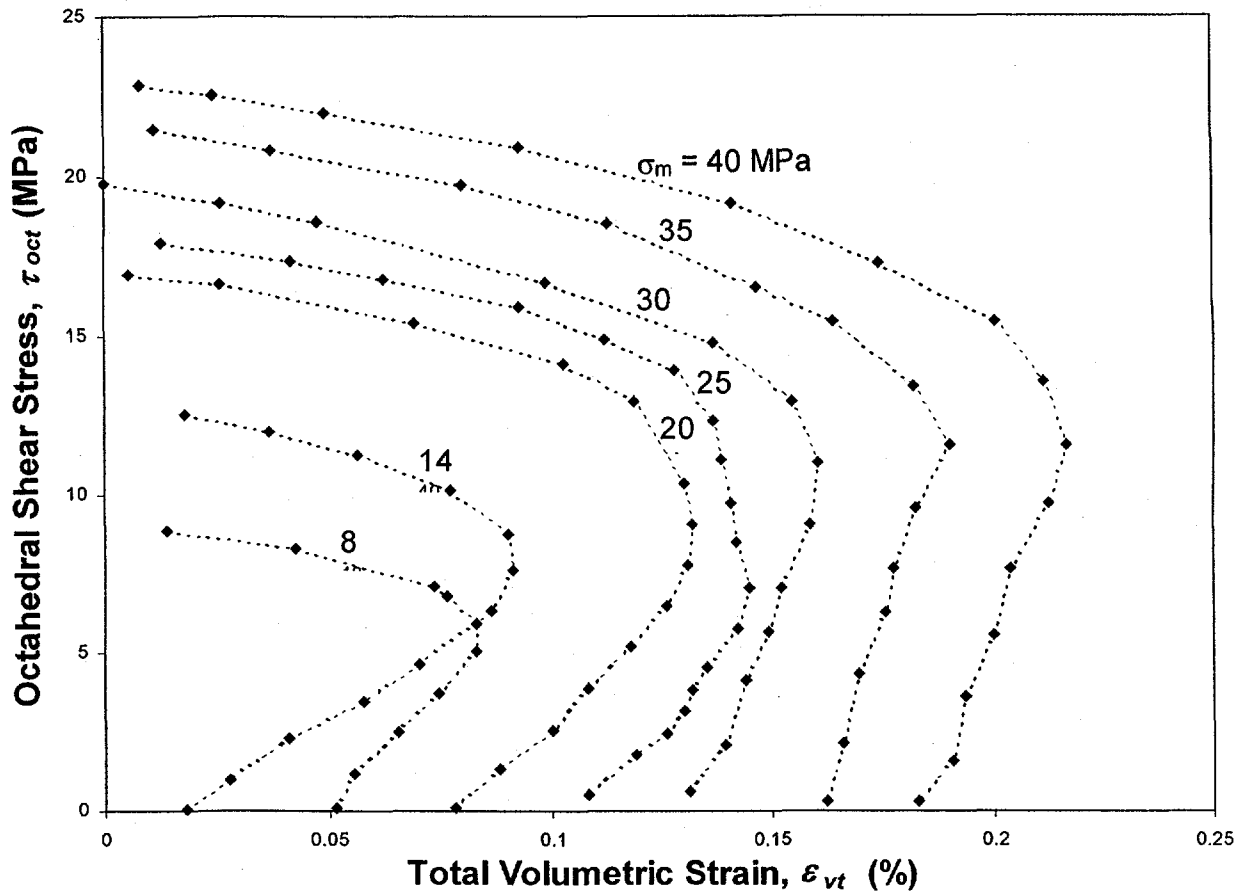


Figure 2. Octahedral Shear Stress vs. Total Volumetric Strain at Various Mean Stresses (Taken from Cristescu & Hunsche 1998)

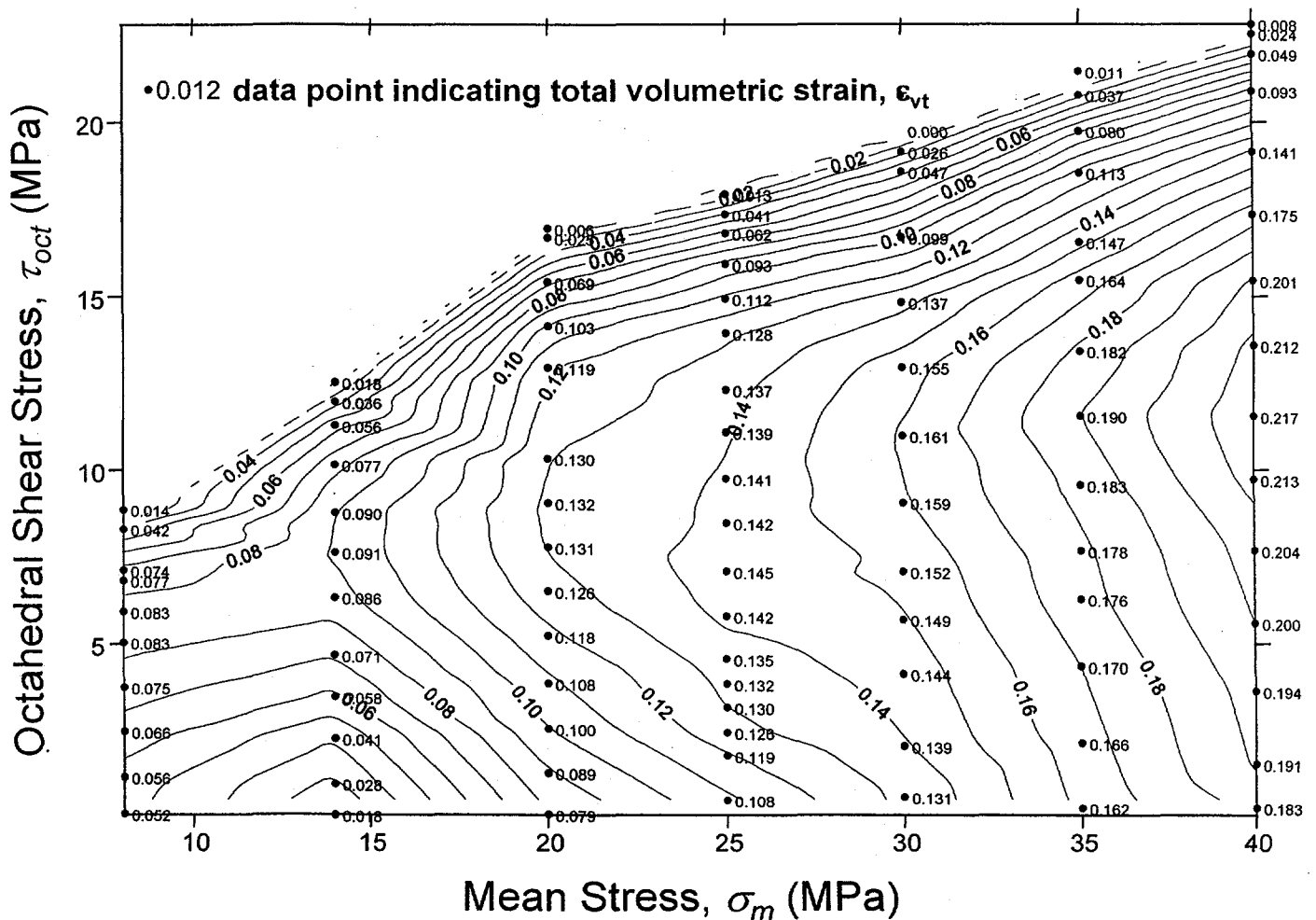


Figure 3. Contour Plot of Total Volumetric Strain as a Function of both Mean Stress and Octahedral Shear Stress (Derived From Cristescu & Hunsche 1998).



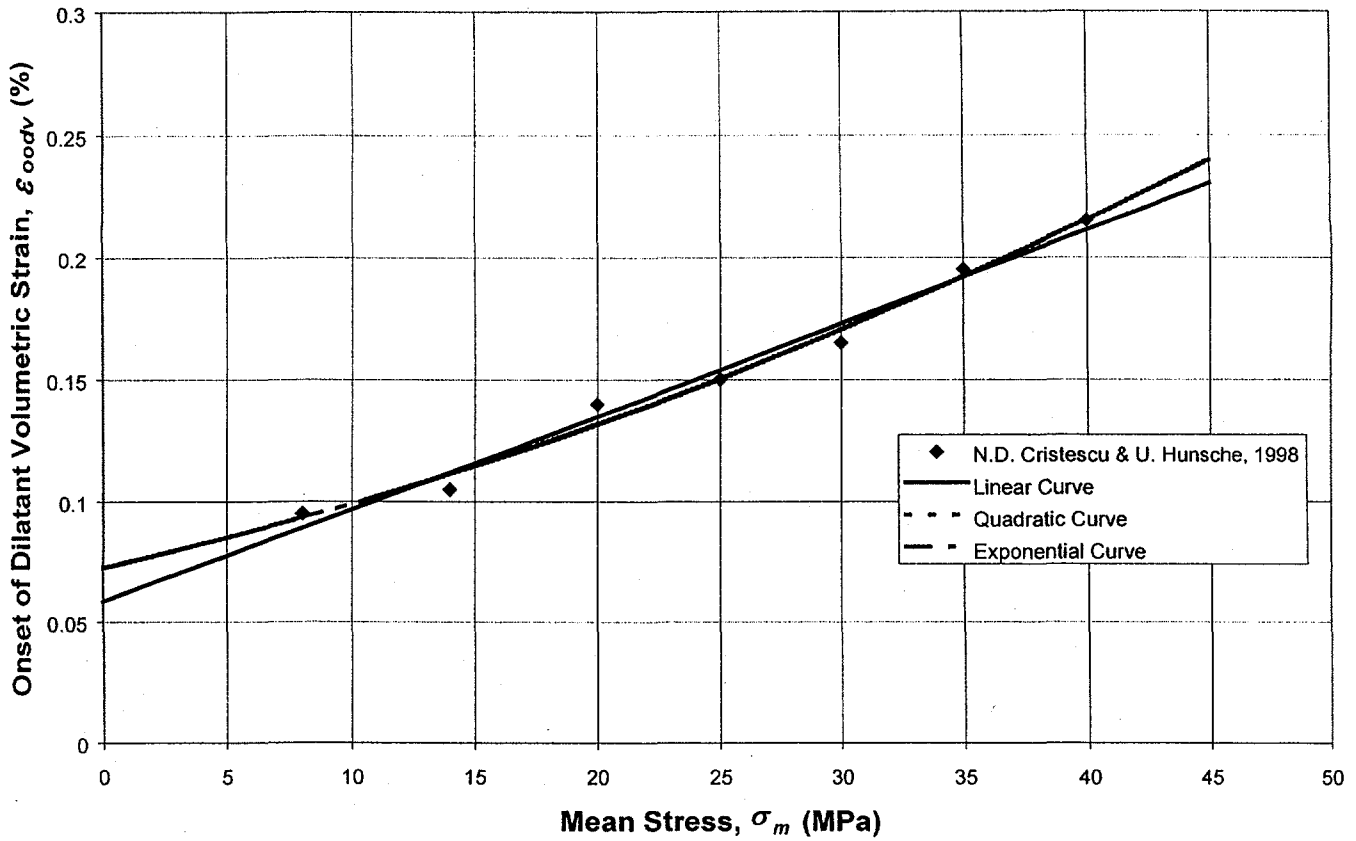


Figure 4. Onset of Dilatant Volumetric Strain vs. Mean Stress ( $\epsilon_{oodv}$  vs.  $\sigma_m$ )

Table 1. Data Fitting Functions for Permeability vs. Dilatant Volumetric Strain

Source	Functional Formulation	Empirical Formula Fit Constants
Blankenship (1996)	$k_1 = A_1 \exp(B_1 \cdot (\epsilon_{dv})^{C_1})$	$A_1 = 7.25 \times 10^{-20}, B_1 = 27.76, C_1 = 0.1573$
Peach (1991)	$k_2 = A_2 (\epsilon_{dv})^{C_2}$	$A_2 = 2.13 \times 10^{-8}, B_2 = 0.0, C_2 = 3$
Stormont-RESPEC (1995)	$k_3 = A_3 \exp(B_3 \cdot (\epsilon_{dv})^{C_3})$	$A_3 = 2.955 \times 10^{-21}, B_3 = 49.90, C_3 = 0.3160$

Table 2. Total volumetric strain ( $\epsilon_{vt}$ ) vs. mean and octahedral shear stress ( $\sigma_m$  and  $\tau_{oct}$ )

$\sigma_m$ (MPa)	$\tau_{oct}$ (MPa)	$\epsilon_{vt}$ (%)	$\sigma_m$ (MPa)	$\tau_{oct}$ (MPa)	$\epsilon_{vt}$ (%)	$\sigma_m$ (MPa)	$\tau_{oct}$ (MPa)	$\epsilon_{vt}$ (%)
40	22.830	0.008	30	16.685	0.099	20	12.964	0.119
40	22.553	0.024	30	14.824	0.137	20	10.341	0.130
40	21.969	0.049	30	12.964	0.155	20	9.065	0.132
40	20.891	0.093	30	11.004	0.161	20	7.788	0.131
40	19.139	0.141	30	9.065	0.159	20	6.522	0.126
40	17.338	0.175	30	7.076	0.152	20	5.245	0.118
40	15.458	0.201	30	5.700	0.149	20	3.879	0.108
40	13.597	0.212	30	4.137	0.144	20	2.583	0.100
40	11.559	0.217	30	2.078	0.139	20	1.316	0.089
40	9.718	0.213	30	0.614	0.131	20	0.099	0.079
40	7.679	0.204	25	17.932	0.013	14	12.538	0.018
40	5.601	0.200	25	17.348	0.041	14	11.984	0.036
40	3.642	0.194	25	16.804	0.062	14	11.291	0.056
40	1.564	0.191	25	15.923	0.093	14	10.143	0.077
40	0.287	0.183	25	14.933	0.112	14	8.768	0.090
35	21.475	0.011	25	13.944	0.128	14	7.620	0.091
35	20.782	0.037	25	12.331	0.137	14	6.333	0.086
35	19.743	0.080	25	11.103	0.139	14	4.661	0.071
35	18.555	0.113	25	9.748	0.141	14	3.474	0.058
35	16.556	0.147	25	8.481	0.142	14	2.286	0.041
35	15.477	0.164	25	7.086	0.145	14	0.980	0.028
35	13.439	0.182	25	5.809	0.142	14	0.069	0.018
35	11.578	0.190	25	4.562	0.135	8	8.857	0.014
35	9.560	0.183	25	3.859	0.132	8	8.293	0.042
35	7.679	0.178	25	3.177	0.130	8	7.125	0.074
35	6.294	0.176	25	2.474	0.126	8	6.828	0.077
35	4.354	0.170	25	1.801	0.119	8	5.938	0.083
35	2.177	0.166	25	0.524	0.108	8	5.057	0.083
35	0.287	0.162	20	16.952	0.006	8	3.761	0.075
30	19.792	0.000	20	16.675	0.025	8	2.494	0.066
30	19.139	0.026	20	15.418	0.069	8	1.188	0.056
30	18.575	0.047	20	14.151	0.103	8	0.099	0.052

Table 3. Onset of Dilatant Volumetric Strain ( $\epsilon_{oodv}$ ) at  $\tau_{oct}$  and  $\sigma_m$ 

$\sigma_m$ (MPa)	$\epsilon_{oodv}$ (%)	$\tau_{oct}$ (MPa)
8.0	0.095	5.0
14.0	0.105	7.5
20.0	0.140	9.0
25.0	0.150	10.0
30.0	0.165	11.0
35.0	0.195	11.5
40.0	0.215	12.0

Table 4. Data Fitting Function for the Onset of Dilatant Volumetric Strain

Type	Functional Formulation	Empirical Formula Fit Constants
Linear	$\epsilon_{oodv} = A_1 + B_1 \cdot \sigma_m$	$A_1 = 5.852 \times 10^{-2}, B_1 = 3.811 \times 10^{-3}$
Quadratic	$\epsilon_{oodv} = A_2 + B_2 \cdot \sigma_m + C_2 \cdot \sigma_m \cdot \sigma_m$	$A_2 = 7.244 \times 10^{-2}, B_2 = 2.371 \times 10^{-3}, C_2 = 2.997 \times 10^{-5}$
Exponential	$\epsilon_{oodv} = \exp(A_3 + B_3 \cdot \sigma_m + C_3 \cdot \sigma_m \cdot \sigma_m)$	$A_3 = -2.621, B_3 = 3.222 \times 10^{-2}, C_3 = -1.272 \times 10^{-4}$